

This article was downloaded by: [Tomsk State University of Control Systems and Radio]

On: 23 February 2013, At: 03:28

Publisher: Taylor & Francis

Informa Ltd Registered in England and Wales Registered Number: 1072954

Registered office: Mortimer House, 37-41 Mortimer Street, London W1T 3JH, UK



## Molecular Crystals and Liquid Crystals

Publication details, including instructions for authors and subscription information:

<http://www.tandfonline.com/loi/gmcl16>

## Viscosity Behavior of Liquid Crystals

Brian C. Benicewicz<sup>a</sup>, Julian F. Johnson<sup>a</sup> & Montgomery T. Shaw<sup>b a</sup>

<sup>a</sup> Department of Chemistry and Institute of Materials Science, University of Connecticut, Storrs, Connecticut, 06268, U.S.A.

<sup>b</sup> Department of Chemical Engineering and Institute of Materials Science, University of Connecticut, Storrs, Connecticut, 06268, U.S.A.

Version of record first published: 20 Apr 2011.

To cite this article: Brian C. Benicewicz, Julian F. Johnson & Montgomery T. Shaw (1981): Viscosity Behavior of Liquid Crystals, *Molecular Crystals and Liquid Crystals*, 65:1-2, 111-131

To link to this article: <http://dx.doi.org/10.1080/00268948108076134>

PLEASE SCROLL DOWN FOR ARTICLE

Full terms and conditions of use: <http://www.tandfonline.com/page/terms-and-conditions>

This article may be used for research, teaching, and private study purposes. Any substantial or systematic reproduction, redistribution, reselling, loan, sub-licensing, systematic supply, or distribution in any form to anyone is expressly forbidden.

The publisher does not give any warranty express or implied or make any representation that the contents will be complete or accurate or up to

date. The accuracy of any instructions, formulae, and drug doses should be independently verified with primary sources. The publisher shall not be liable for any loss, actions, claims, proceedings, demand, or costs or damages whatsoever or howsoever caused arising directly or indirectly in connection with or arising out of the use of this material.

# Viscosity Behavior of Liquid Crystals

BRIAN C. BENICEWICZ,<sup>†</sup> JULIAN F. JOHNSON

*Department of Chemistry and Institute of Materials Science,*

*and*

MONTGOMERY T. SHAW

*Department of Chemical Engineering and Institute of Materials Science,  
University of Connecticut, Storrs, Connecticut 06268, U.S.A.*

*(Received March 21, 1980)*

The literature on the viscosity behavior of liquid crystals is reviewed with emphasis on the experimental results. These results are discussed in terms of the mesophase structure. Discussion of polymeric liquid crystals has been excluded since they have recently been reviewed.

## INTRODUCTION

This review covers the literature on the viscosity behavior of liquid crystals from 1972 to mid-1979. The last review dealing with this subject is over ten years old.<sup>1</sup> Research in the area of polymeric liquid crystals has grown recently largely on account of their application in producing high-modulus, high-strength fibers. This class of materials will not be covered here since there is a recent review which thoroughly examines this area.<sup>2</sup>

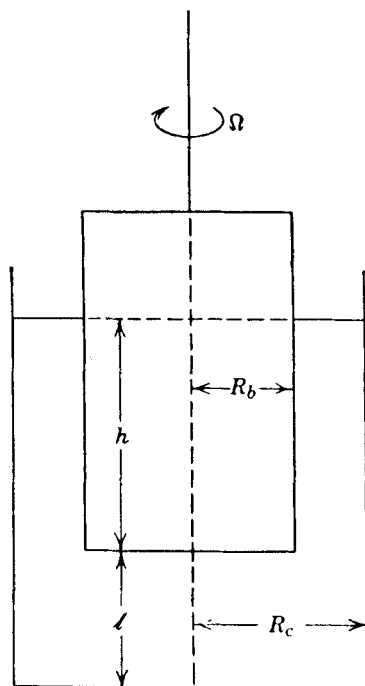
There are many ways that viscosities are measured and a section describing some of the methods is included. The reader is referred to literature specifically dealing with the measurement of viscosities for a more complete coverage.<sup>3,4</sup>

## DEFINITION OF TERMS

For all rotational viscometers, the two quantities measured are rate of rotation and torque. In the concentric cylinder geometry, shown schematically in Figure 1, the sample is placed between two cylinders with a specified

---

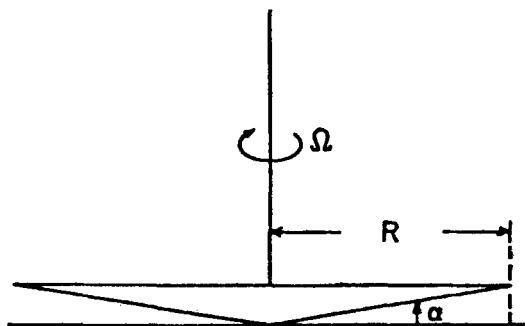
<sup>†</sup> Current address: Celanese Research Co., Summit, N.J., U.S.A.

FIGURE 1 Concentric cylinder viscometer of the Searle type.<sup>3</sup>

gap distance. One of the cylinders is rotated at a controlled rate which is proportional to the shear rate. The torque measured is proportional to the shear stress. The apparent viscosity of the fluid is defined as the ratio of shear stress to the shear rate. For simple or Newtonian fluids the viscosity is independent of the shear stress. However, for non-Newtonian fluids the viscosity is a function of the shear stress.

In the cone and plate geometry shown in Figure 2, the cone is rotated at a controlled rate and the torque is measured on the flat plate. The attractive characteristic of the cone and plate viscometer is that the shear stress and shear rate are essentially independent of the radius,  $R$ , at low cone angles. This is true in the case of the concentric cylinder viscometers only for small gap widths. The cone and plate viscometer can be adapted for rheo-optical studies by replacing the cone and plate by a pair of parallel glass platens. This is very useful for correlating viscosity behavior with transitions and textures.

In the rotating field technique the sample is enclosed in a container which is placed in a magnetic field. As the magnetic field is slowly rotated the torque produced by the liquid crystalline fluid on the container is measured.


 FIGURE 2 Cone and plate viscometer.<sup>4</sup>

Rotational viscometers are used to measure both steady-state, as just described, and dynamic properties of liquid crystals. These viscometers are adapted to dynamic measurements by producing an oscillating rotational shear instead of a steady rotating shear.

The falling ball viscometer measures the time for a ball to fall through the test fluid. This type of viscometer can be made from a graduate cylinder with a rubber stopper having a glass tube in it for insertion of the balls. The balls can be small ball bearings or a set may be purchased, the members of which are made of different materials. By using calibrated balls of different sizes in the same glass cylinder, tests can be performed over a wide viscosity range.

A capillary viscometer is shown in Figure 3. With this viscometer, the time  $t$  required for a volume  $V$  to flow through the capillary of length  $L$  and radius  $r$  is measured. The Newtonian viscosity is calculated from the Poiseuille equation

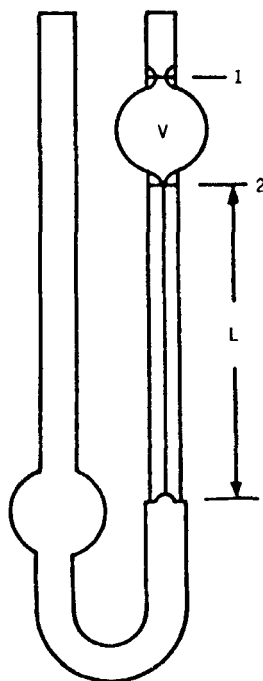
$$\eta = \frac{\pi r^4 t P}{8 L V}$$

where  $P$  is the applied pressure differential defined as:

$$P = h g \rho$$

where  $h$  is the average height of the liquid in the tube,  $g$  is the acceleration due to gravity and  $\rho$  is the density of the liquid. Capillary viscometers are used in this manner to determine absolute viscosities. Since it is difficult to determine the absolute dimensions of a fine capillary, the flow time for a liquid of known viscosity is determined and a viscometer constant  $C$  is measured. A kinematic viscosity,  $\eta_k$ , is then calculated using the equation:

$$\eta_k = C t \quad C = \frac{h \pi r^4 g}{8 L V}$$

FIGURE 3 Ostwald capillary viscometer.<sup>4</sup>

A more precise form of this equation that is often used is the following;

$$\eta_k = Ct - \frac{B}{t}$$

The constant  $B$  is a term which corrects for the kinetic energy effects. It is either calculated or determined by calibrating with standards of known different viscosities. If the flow times of the viscometer are 200 seconds or more, the kinetic energy correction is small enough so that precise determination of  $B$  is not required. For non-Newtonian fluids, additional corrections must be made to account for the non-parabolic velocity profile in the capillary.

Ultrasonic wave propagation is also used to investigate the viscosities of liquid crystals. Measurements of the attenuation anisotropy are used to determine values of the five viscosity coefficients found in the equation describing the attenuation in an anisotropic fluid. There are current reviews covering the contribution of ultrasonic measurements to the study of liquid crystals.<sup>5-7</sup>

There have been new methods developed to measure viscosities of anisotropic fluids. A new type of viscometer has been described which utilizes a

steel tuning fork capable of measuring a large range of viscosities.<sup>8</sup> The viscometer was calibrated and tested with glycerin-water solutions and, although no measurements were performed on liquid crystals, the possibility was stated.

The rotational or twist viscosity of the nematic *p*-methoxybenzylidene-*p*-*n*-butylaniline (MBBA) was determined by a new optical method.<sup>9</sup> The liquid crystal was held between parallel glass plates and oriented so that the director was in a plane perpendicular to the axis of the incident light cone. The rotation angle of the interference figure was monitored as the top plate was rotated and a twist viscosity was calculated through use of a simple equation.

## ORIENTATION

The orientation of the molecules in an anisotropic liquid is important in defining their rheological properties. There may be a several-fold difference in viscosity for different orientations of the same liquid crystal at the same temperature. It is important to note that shear tends to align the molecules of an anisotropic liquid in the direction of shear flow and care must be used to insure the desired orientation.

The data in Table I show the viscosities for the three principal orientations in simple-shear flow experiments; these are normally referred to as Miesowicz viscosities.<sup>10</sup> The three orientations, which are commonly achieved by using a magnetic field, are shown schematically in Figure 4. Caution must be used when reviewing the literature as the orientations 1, 2, 3 are not universally defined as such and may be defined as 2, 1, 3 by another author. In this review, the definitions found in Table I will be used or the

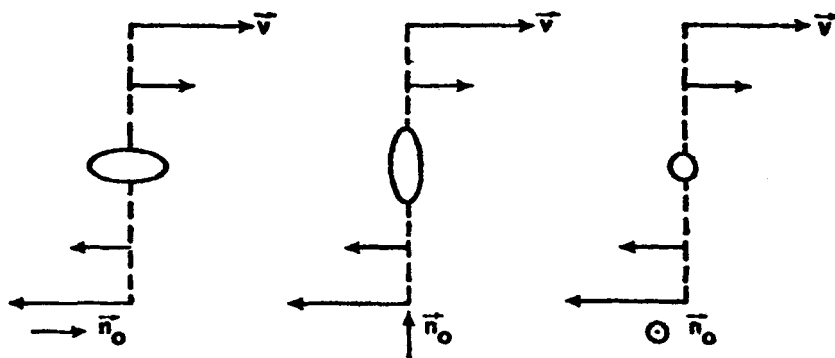


FIGURE 4 Definition of the Miesowicz viscosities showing relative orientation of the preferred axis ( $\vec{n}_0$ ),  $\vec{v}$  and the velocity gradient.<sup>32</sup>

TABLE I  
Nematic viscosities for the three principal orientations<sup>1,0</sup>

Substance and temperature	Molecules parallel to the direction of flow $\eta_1$	Molecules parallel to the gradient of velocity $\eta_2$	Molecules perpendicular to the direction of flow and to the velocity gradient $\eta_3$
<i>p</i> -Azoxyanisole, 122°C	0.024 $\pm$ 0.0005	0.092 $\pm$ 0.004	0.034 $\pm$ 0.003
<i>p</i> -Azoxyphenetole, 144.4°C	0.013 $\pm$ 0.0005	0.083 $\pm$ 0.004	0.025 $\pm$ 0.003



orientation will be defined in terms of the long molecular axis and flow field.

There are several methods which are used to achieve different orientations. These include the use of electric fields, magnetic fields, rubbing of glass or quartz surfaces and precipitation of a material on the surfaces exposed to the liquid crystals. The rubbing method involves cleaning the glass or quartz surfaces with, for example, chromic acid and then rubbing these surfaces with a cleaning tissue.<sup>12</sup> This results in aligning the molecules of the liquid crystal with their long axes parallel to the direction of rubbing.

The precipitation method requires the deposition of a material such as lecithin onto the surfaces exposed to the liquid crystals. This is done by painting the surfaces with a dilute solution of lecithin in a solvent that vaporizes quickly, leaving a thin film. The lecithin thus deposited aligns the molecules perpendicular to the surfaces.

## SMECTICS

The dynamic rotational viscosity in the smectic-C and nematic mesophases of heptyloxyazoxybenzene has been determined by measuring the mechanical dissipation in the liquid crystalline phases during oscillation in a magnetic field.<sup>13</sup> The molecules within the smectic layers had no long range positional order and could reorient about the axis perpendicular to the layers. This motion was characterized by a rotational viscosity. An Arrhenius plot of the viscosity is shown in Figure 5. There was a noticeable drop in viscosity at the nematic to smectic-C transition which was accompanied by a drop in activation energy from  $54.9 \text{ J mole}^{-1}$  at the lower temperatures of the nematic phase to  $20.4 \text{ J mole}^{-1}$  for the smectic-C phase.

Dynamical rotational measurements were also made on terephthal-bis-butylaniline (TBBA) which exhibits a nematic and several smectic mesophases.<sup>14</sup> The viscous energy dissipation was the quantity measured as the liquid crystal was oscillated in a magnetic field and its behavior as a function of temperature was used to describe the structure of the various mesophases.

The rotational viscosity of the smectic-A phase of *p*-*n*-octyl-*p*'-cyanobiphenyl has been determined by use of a transparent cone and plate apparatus which allowed inspection of the shear textures.<sup>15</sup> The surfaces were treated with lecithin to obtain a homeotropic alignment, i.e., the smectic layers were parallel to the surfaces. This is of course impossible since the surfaces of a cone and plate rheometer are not parallel, but at low angles this condition is approached. A planar shear flow cell was constructed using glass microscope slides to better observe the various textures. A disordered focal conic texture created by shear was observed and the apparent viscosity increased with

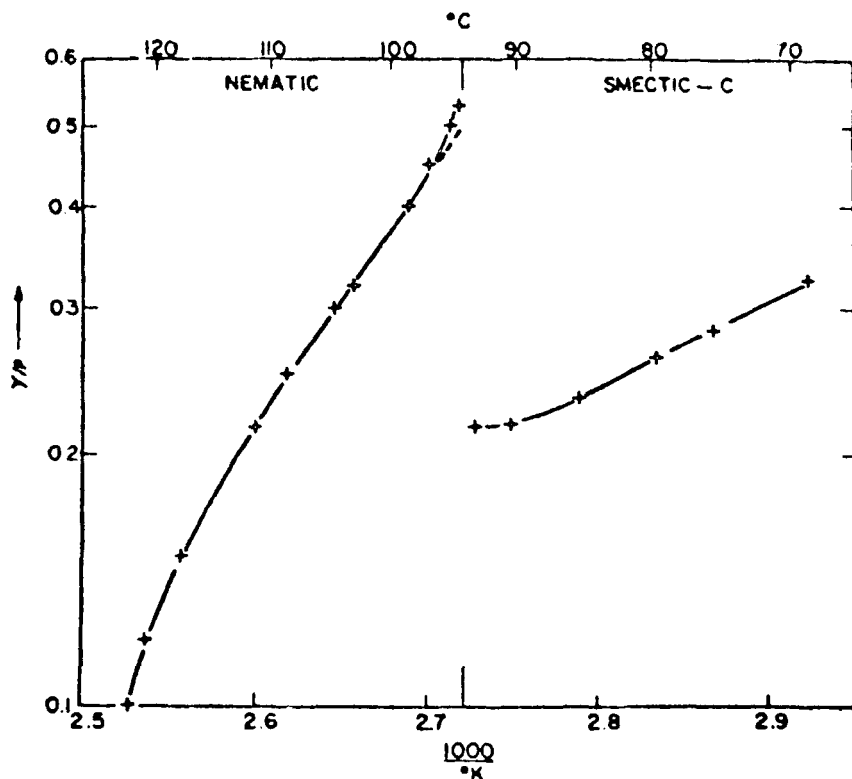


FIGURE 5 Arrhenius plot of the rotational viscosity through the nematic, smectic-C transition. The quantity plotted  $\gamma/\rho$ , the kinematic viscosity in cgs units, or stokes;  $\gamma$  is in poises and  $\rho$  is the density of the liquid crystal.<sup>13</sup>

the fraction of sample that contained this texture. The viscosity corresponding to the flow of the smectic layers sliding over one another was 1.2 poise. It was suggested that a finite yield stress may exist.

Kim, *et al.*<sup>16</sup> have measured the shear viscosity of *p*-cyanobenzylidene-*p*'-*n*-octyloxyaniline (CBOOA) by observing the flow through a slit. Near-Newtonian behavior was observed when the smectic planes were oriented parallel to the slit plates and the temperature dependence followed an Arrhenius behavior. The flow was non-Newtonian when the smectic planes were parallel to the velocity and velocity gradient. These measurements were reproducible only if the sample was run back and forth through the slit before each experiment to eliminate surface effects.

The flow properties of smectic liquid crystals were measured using a rotational viscometer at shear rates from 10 to 500  $\text{sec}^{-1}$ .<sup>17,18</sup> The ammonium salts of myristic, palmitic, stearic and oleic acids were used in the

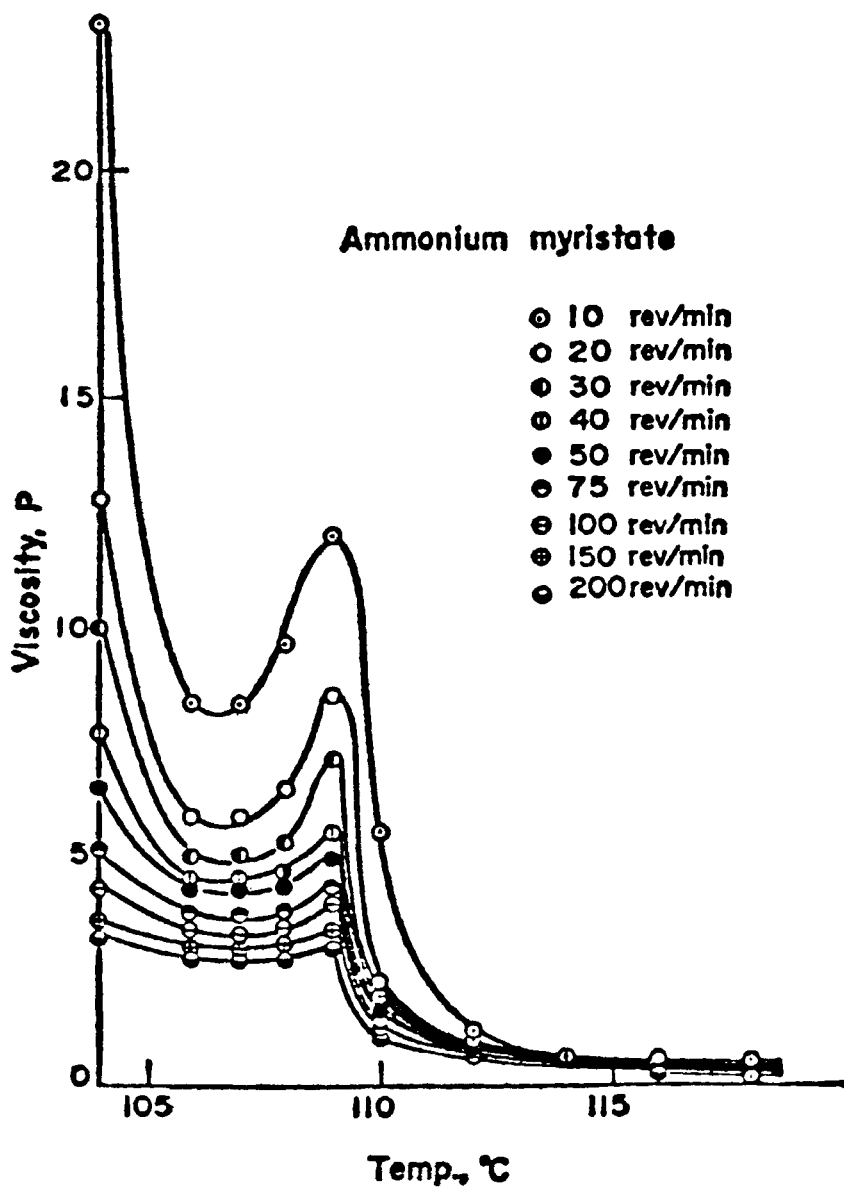


FIGURE 6 Relation between viscosity and temperature at various shear rates for ammonium myristate.<sup>17</sup>

investigation. The flow in the smectic phase was generally non-Newtonian and the viscosity versus temperature curves exhibited a sharp maximum, the height of which was dependent on the shear rates as shown in Figure 6. The flow behavior was qualitatively explained in terms of the translational and rotational motions of the molecules in the liquid crystalline state.

The flow behavior of the thermotropic and lyotropic mesophases of ammonium dodecanoate were determined and compared using a rotational viscometer at shear rates from 80–600  $\text{sec}^{-1}$ .<sup>19</sup> The activation energy of flow for the thermotropic mesophase ( $\sim 130 \text{ kcal mol}^{-1}$ ) was more than ten times that of the lyotropic mesophase ( $\sim 6\text{--}12 \text{ kcal mol}^{-1}$ ) indicating a greater temperature dependence of viscous flow for the thermotropic mesophase. The activation energy for the thermotropic mesophase changed sign at a temperature corresponding to a maximum in the apparent viscosity versus temperature curve. The lyotropic mesophase did not exhibit an anomaly over the temperature range of the experiments. The problems of comparing the two systems were discussed and the possibility of a comparison between lyotropic mesophases and colloidal systems as being more meaningful was cited.

## CHOLESTERICIS

The non-Newtonian viscosity of cholesteryl oleyl carbonate (COC) was investigated using a concentric cylinder viscometer at shear rates from 0.1 to 70  $\text{sec}^{-1}$ .<sup>20</sup> A maximum in the apparent viscosity occurred at the cholesteric-isotropic transition which was characterized by non-Newtonian behavior. The flow curves for the cholesteric mesophase were almost linear indicating Newtonian behavior. However, at lower shear rates of 0.1–1  $\text{sec}^{-1}$ , a non-linear or non-Newtonian behavior resulted. This suggests that the cholesteric structure breaks down at fairly low shear stresses and the near Newtonian behavior at higher shear rates occurs due to the existence of the second Newtonian range. The activation energies for viscous flow in the isotropic liquid were 14.0  $\text{kcal mol}^{-1}$  at shear rates of 0.1  $\text{sec}^{-1}$  and 25  $\text{sec}^{-1}$ . In the cholesteric phase the activation energy obtained at 0.1  $\text{sec}^{-1}$  (26.1  $\text{kcal mol}^{-1}$ ) was higher than that obtained at 25  $\text{sec}^{-1}$  (16.8  $\text{kcal mol}^{-1}$ ).

The viscosity of COC in the cholesteric phase was only slightly different than the viscosity in the isotropic phase.<sup>21</sup> The isotropic isotherm of the  $\log \eta$  versus pressure diagram, extended into the cholesteric region, was just lower than the cholesteric isotherm. A sharp peak in the viscosity at the transition increased with increasing pressure. It was concluded that coupling between the cholesteric layers was stronger than that between the molecules within the layers.

The viscosities of several cholesteric liquid crystals, measured at low shear rates of  $0.1$  to  $10 \text{ sec}^{-1}$ , exhibited large increases in viscosity at the isotropic to cholesteric transition.<sup>22</sup> The large viscosities measured using the falling ball technique were due, in part, to the turbulent flow that was produced in this type of viscometer. A substance in the cholesteric phase can exhibit two very different viscosities depending on whether the flow direction is parallel to perpendicular to the plane of the layers. The falling ball viscometer used at low shear rates probably measured a viscosity that is a combination of these two orientations. The viscosity behavior of the three liquid crystals, cholesteryl linoleate (CL), cholesteryl oleate (CO), and cholesteryl linolenate (CLn), in the isotropic phase, was Newtonian with an activation energy of  $4.8 \text{ kcal mol}^{-1}$ . The viscosity of CL and CLn was lower than that of CO. The larger degree of unsaturation of cis-isomers caused a decrease in flexibility and a reduction in overall length of the acyl chain thereby reducing the ability of the molecules to interfere with the flow of adjacent molecules.

Porter *et al.*<sup>23</sup> measured the viscosities of mesophase blends of cholesteryl acetate and cholesteryl myristate as a function of composition, shear rate and temperature in the smectic, cholesteric and isotropic phases. Measurements were made using a cone and plate viscometer at shear rates of  $0.034$ ,  $3.4$  and  $34 \text{ sec}^{-1}$ . A viscosity maximum was observed near the isotropic-cholesteric transition; however, the non-Newtonian cholesteric viscosities for all compositions were virtually the same, within experimental precision, at the same shear rates. This was interpreted to mean that the esters were rheologically and thermodynamically the same and the cholesteric mesophase was due solely to the arrangement of the steroid moiety. The cholesteric-smectic transition was accompanied by a sharp rise in viscosity, followed by a leveling off or slight continuous increase in viscosity throughout the smectic phase. This behavior is shown in Figure 7. A break in viscosity, which may be due to a textural change, was detected for most samples on the lower temperature side of the cholesteric-isotropic transition.

It was predicted by Leslie<sup>24</sup> that capillary shear flow should be Newtonian for cholesteric liquid crystals when the flow direction is perpendicular to the helix axis. This was observed in a mixture of cholesteryl chloride and cholesteryl myristate,  $1.65:1$  by weight, in a slit at shear rates of approximately  $10 \text{ sec}^{-1}$ .<sup>25</sup> Orientation was maintained by rubbing the surfaces and use of a magnetic field. Newtonian flow was observed on both sides of the isotropic-cholesteric transition in contrast to the strong non-Newtonian behavior observed with unoriented samples.

Cholesteric liquid crystals can exhibit shear-induced textural changes. These textural changes can be associated with changes in the rheological behavior of the fluid.<sup>26,27</sup> For mixtures of COC and cholesteryl chloride

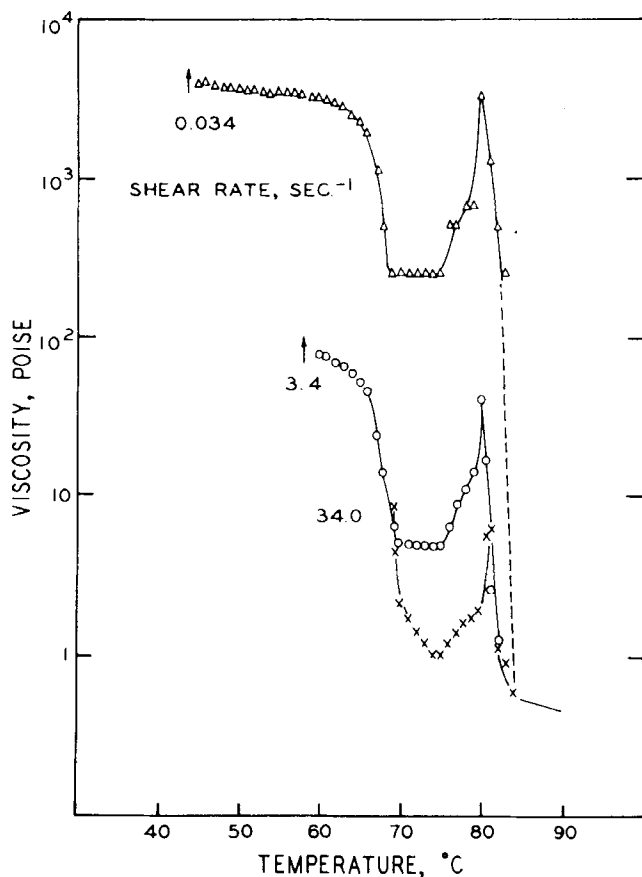


FIGURE 7 Change in viscosity with temperature for a 91.4/8.6 mixture of cholesteryl myristate/acetate.<sup>23</sup>

(CCI), the textures have been related to the flow behavior (in order of increasing shear) as Grandjean (non-Newtonian), focal conic (Newtonian), and homeotropic (non-Newtonian). A rotational viscometer with a set of large-radius glass platens allowed observation of the textures at higher shear rates than possible with a cone and plate configuration. At low shear rates, the cholesteric helices acted as long rigid rods with length greater than the pitch. At higher shear rates, a critical shear energy was reached which overcame the molecular cohesive forces in the helices and fragmented the helices. Normal force measurements showed a decrease in size of molecular clusters with increasing shear rate. It was predicted that an isotropic liquid would result at the limit of very high shear under isothermal conditions.

The helix structure of COC was unwound to a birefringent texture at a critical shear rate of  $1.5 \times 10^3 \text{ sec}^{-1}$ .<sup>28</sup> The change in structure was discontinuous in contrast to the transition to an unwound structure caused by an external field. The value for the critical shear rate was comparable to that reported for the focal conic-homeotropic transition for a 23/77 weight percent mixture of CCl/COC.<sup>26</sup>

## NEMATICS

A continuum theory describing the hydrodynamic properties of a nematic liquid crystal was formulated by Ericksen<sup>29</sup> and Leslie.<sup>30</sup> The stresses produced in a nematic during shear depend on the relative orientation of the nematic axis and may be asymmetric, thus producing a torque. The dissipative stress tensor, as proposed by Leslie, contains five independent coefficients with dimensions of viscosity. The viscosities measured in simple shear flow experiments are some linear combination of the viscosity coefficients. The temperature dependence of the coefficients was investigated experimentally and equations were derived to explain the effect of temperature and shear on the viscosities of liquid crystals.<sup>31-38</sup> However, more work is still required for a satisfactory quantitative explanation, as different sets of data present varying degrees of confirmation to the theories.<sup>39</sup>

The three principal or Miesowicz viscosities of MBBA are shown in Figure 8.<sup>40</sup> These were determined by a novel procedure which measured the flow velocity and the change in birefringence induced by laminar flow through a duct of rectangular cross section. Measurements were also made on *p*-*n*-hexyloxybenzylidene-*p*'-aminobenzonitrile (HBAB) and a 1:1:1 molar mixture of HBAB with *p*-*n*-butoxybenzylidene-*p*'-aminobenzonitrile and *p*-*n*-octanoyloxybenzylidene-*p*'-aminobenzonitrile which exhibited similar behavior. Low flow velocities were used so that the measured viscosities were independent of the shear rate. The viscosities of the 1:1:1 mixture were essentially identical to those measured for HBAB at the same temperature. This was a reasonable observation as the three components in the mixture were chemically similar and the molecular interaction did not change when one kind of molecule was replaced by another.

Summerford, *et al.*<sup>11</sup> have also measured two of the Miesowicz viscosities of MBBA and found that their results disagreed with earlier studies. The experimental method consisted of measuring the force on a thin vane suspended in a container of liquid as the container was lowered at a constant rate. This motion produced a known velocity gradient in the fluid, while the force on the vane provided the shear stress. One of the main advantages was that the effects of flow alignment were minimized by using an extremely

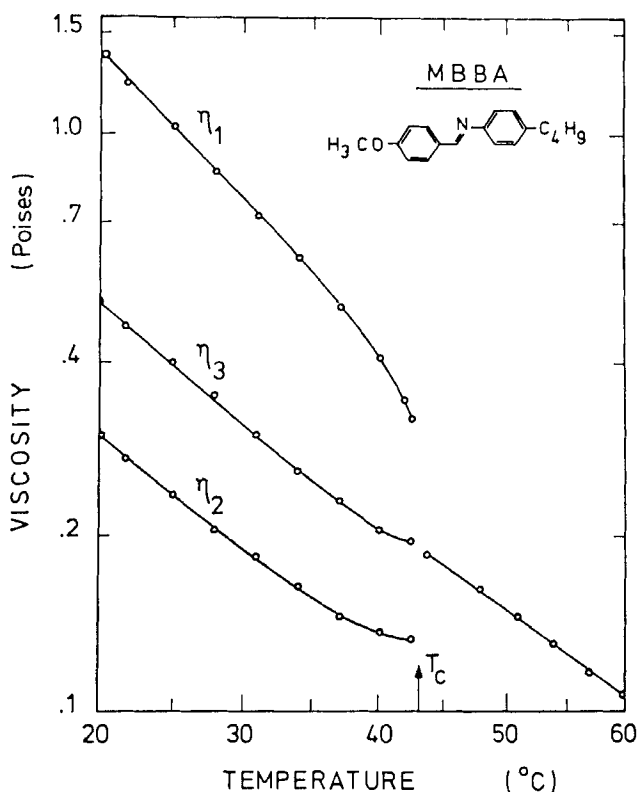


FIGURE 8 The viscosity coefficients  $\eta_1$ ,  $\eta_2$ , and  $\eta_3$  of MBBA as function of temperature. The temperature scale is linear in  $T^{-1}$ .  $\eta_1$  and  $\eta_2$  are defined in reverse of the definitions in Table I.<sup>40</sup>

small shear rate in a bulk sample. The viscosities were higher by about 0.30 poise than those of Gahwiller.<sup>40</sup> It is interesting to note that this was also true of the isotropic phase where the viscosity is Newtonian and independent of shear rate. By using a magnetic field to orient the liquid crystals, the viscosity was defined as a function of the angle,  $\phi$ , between the direction of velocity gradient and the projection of the director  $\mathbf{n}$  onto the plane perpendicular to the flow. These results are shown in Figure 9 where the solid curve is the predicted behavior and the dots are data points.

White *et al.*<sup>41</sup> detected a discontinuity in the apparent viscosity of HBAB at  $\sim 91^\circ\text{C}$  with a falling ball viscometer. At this temperature the flow properties changed from those normally found in a nematic with molecular alignment, to a regime in which molecular alignment was not observed. The apparent viscosity was very close to the viscosity when the director was



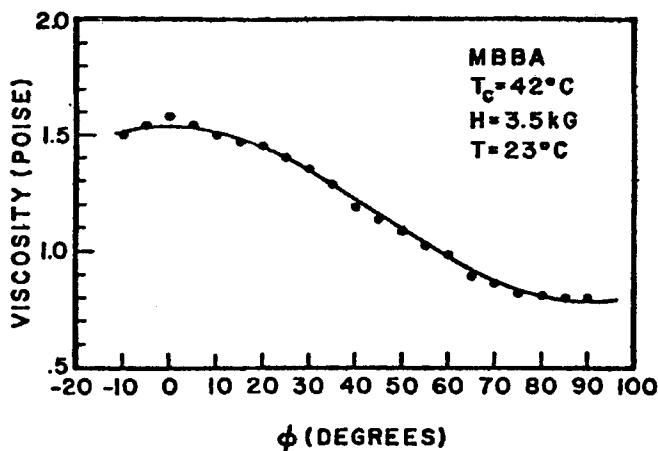


FIGURE 9 Measured viscosity coefficient of MBBA as a function of the angle  $\phi$ . See text for explanation.<sup>11</sup>

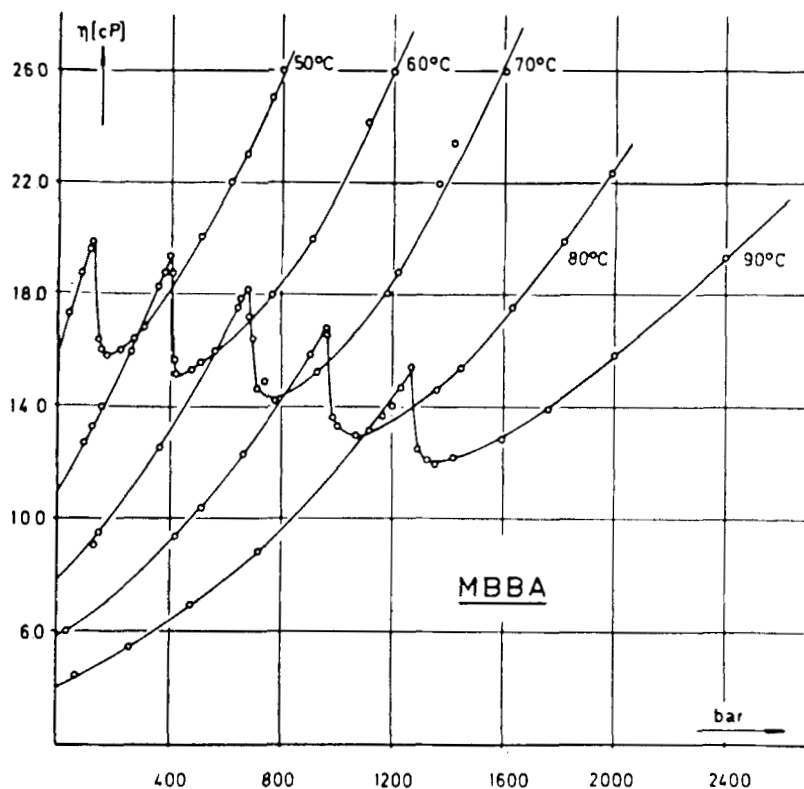
parallel to the velocity vector. However, measurements with a Ostwald-Poiseuille viscometer did not reproduce the discontinuity.

The kinematic viscosity of 24 nematic liquid crystals was measured by Flanders<sup>42</sup> as a function of temperature using the rotating magnetic field technique. Results were also given for the activation energy of viscous flow. Data from earlier studies were used to calculate the twist viscosity of eight nematics.<sup>43</sup>

The rotational viscosity of three nematic liquid crystals has been reported in a study that disagrees with an earlier report on the flow-alignment angle of the three nematics.<sup>44</sup>

The effect of an electric field on viscosity was demonstrated when the flow speed of a nematic liquid crystal was measured as a function of the strength of an electric field applied perpendicular to the flow direction in a slit.<sup>45</sup> The flow speed changed across a narrow voltage range as the long axis of the molecules was oriented perpendicular to the flow direction.

Kuss<sup>21,46</sup> has investigated the viscosity-pressure behavior of two nematic liquid crystals using a high temperature and pressure falling ball viscometer. The viscosity-pressure behavior for MBBA is shown in Figure 10. The nematic to isotropic transition was characterized by a sharp peak in the viscosity-pressure isotherm. The nematic phase had a lower viscosity but a higher density than the isotropic phase. This was due to the nearly parallel orientation of the molecules in the nematic phase allowing them to pack close to each other and yet flow more easily past each other than in the isotropic phase. Differences in the viscosity-pressure behavior of MBBA

FIGURE 10 The viscosity pressure isotherms of MBBA.<sup>46</sup>

and *p*-ethoxybenzylidene-*p'*-*n*-butylaniline (EBBA) were detected and attributed to the different effects that density and temperature had on these liquid crystals.

### PRETRANSITIONAL BEHAVIOR

Considerable attention has been given to pretransitional behavior in the static and dynamic properties of liquid crystals near phase transition regions. These anomalies are described in a phenomenological theory proposed by de Gennes.<sup>47</sup> He compared the nematic to smectic-A transition to the superconducting and liquid helium transitions. Further work on de Gennes' proposal has resulted in the prediction that the twist viscosity of a nematic should behave according to the pretransitional form  $(T - T_c)^{-x}$ .<sup>48,49</sup> The value for the exponent describing this behavior is not yet completely agreed upon.

Pretransitional effects have been detected in the dynamic viscosity of several liquid crystals in the isotropic phase near the isotropic-nematic transition.<sup>50-52</sup> The viscosity displayed a dispersion anomaly in the isotropic phase indicating the presence of a relaxation process associated with the phase transition. When sufficiently far from the transition normal Newtonian behavior is observed in both the isotropic and nematic phases.

A logarithmic divergence of the shear viscosity was detected in the isotropic phase of two cholesteric liquid crystals which exhibit the cholesteric blue phase upon cooling.<sup>53</sup> Measurements on a third cholesteric which did not form the blue phase did not show a pretransitional divergence.

Martins *et al.*<sup>54</sup> have examined much of the existing experimental data on the critical behavior of the twist viscosity,  $\gamma_1(T)$ , near the nematic-smectic-A transition. Using a new analytical approach it is shown that the data agree with the predicted value  $x = 0.33$  for the critical exponent describing the behavior of  $\gamma_1(T)$  above the transition. This supports the helium-analogy theory proposed by de Gennes. The discrepancies arose from the fact that different authors used different empirical equations for the regular term in the expression for  $\gamma_1(T)$ .

Hardouin *et al.*<sup>55</sup> pointed out that existing studies on the critical behavior of  $\gamma_1(T)$  have been performed on pure compounds for which the nematic-smectic-A transition is weakly first order. Measurements were thus performed on binary mixtures of liquid crystals which were strictly second order. A divergence in the twist viscosity was detected near the nematic-smectic-A transition. Interestingly, a divergence was not observed near a nematic-smectic-A-smectic-C singular point.

The rotational and three Miesowicz viscosities were measured for *p*-n-octyloxy-*p*'-cyanobiphenyl by Léger and Martinet.<sup>56</sup> A divergence was detected in  $\gamma$  and  $\eta_1$  near the nematic-smectic-A transition while  $\eta_2$  and  $\eta_3$  exhibited normal behavior. The data supported the helium analog prediction as the value for the critical exponent was  $0.36 \pm 0.05$ . A permeation regime in the smectic phase produced a large viscosity anisotropy,  $\eta_1/\eta_2 \simeq 150$ .

Ultrasonics have also been used to study pretransitional behavior in dynamic properties of liquid crystals. The reader is referred to the reviews<sup>5-7</sup> cited earlier on the use of ultrasonics in the study of liquid crystals for results of this application.

## CONCLUSIONS

It has already been noted<sup>39</sup> that more accurate measurements of the viscosity of liquid crystals are needed. Measurements on other rheological properties other than viscosity are uncommon. The rheological properties of polymeric

liquid crystalline melts are almost unknown for the simple reason that these materials are just being developed. Information in these areas and others would be helpful in understanding both the structure and processing of liquid crystals. Additional work near the transition points and polycritical points might also prove interesting. In general, our understanding of the rheology of liquid crystals is not complete and further work would be welcomed.

### Acknowledgements

Grateful acknowledgement is given to the following for permission to use the figures in this paper: John Wiley and Sons, Inc., for Figures 1 and 3. D. Reidel Publishing Company for Figure 2. Macmillan Journals Ltd., for Table 3. Bangalore Book Printers for Figure 4. American Institute of Physics for Figures 5 and 9. Pergamon Press for Figure 6. Gordon and Breach Science Publishers Ltd., for Figures 7, 8 and 10.

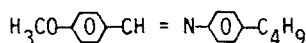
### References

1. R. S. Porter and J. F. Johnson, in *Rheology IV*, ed. F. R. Eirich, Academic Press, New York (1967).
2. D. G. Baird, in *Liquid Crystalline Order in Polymers*, ed. A. Blumstein, Academic Press, New York (1978).
3. J. R. Van Wazer, J. W. Lyons, K. Y. Kim, and R. E. Colwell, *Viscosity and Flow Measurement*, John Wiley and Sons, Inc., New York (1963).
4. J. F. Johnson, J. R. Martin, and R. S. Porter, *Techniques of Chemistry*, Vol. 1—Physical Methods of Chemistry, Part VI: Supplement and Cumulative Index, eds. A. Weissbenger, and B. W. Rossiter, John Wiley and Sons, Inc., New York (1977).
5. S. Candau and S. V. Letcher, in *Adv. Liq. Cryst.*, 3, ed. G. H. Brown, Academic Press, New York (1978).
6. G. G. Natale, *J. Acoust. Soc. Am.*, **63**, 1265 (1978).
7. G. G. Natale, *J. Acoust. Soc. Am.*, **63**, 1677 (1978).
8. P. L. Chung, *Rev. Sci. Instrum.*, **44**, 1669 (1973).
9. P. E. Cladis, *Phys. Rev. Lett.*, **28**, 1629 (1972).
10. M. Miesowicz, *Nature*, **158**, 27 (1946).
11. J. W. Summerford, J. R. Boyd, and B. A. Lowry, *J. Appl. Phys., Phys.*, **46**, 970 (1975).
12. P. Chatelain, *Acta Crystallogr.*, **1**, 315 (1947).
13. S. Meiboom and R. C. Hewitt, *Phys. Rev. Lett.*, **34**, 1146 (1975).
14. S. Meiboom and R. C. Hewitt, *Phys. Rev. A*, **15**, 2444 (1977).
15. R. G. Horn and M. Kleman, *Ann. Phys.*, (3), 229 (1978).
16. M. G. Kim, S. Park, Sr., M. Cooper, and S. V. Letcher, *Mol. Cryst. Liq. Cryst.*, **36**, 143 (1976).
17. B. Tamamushi, *Biorheology*, **10**, 239 (1973).
18. B. Tamamushi, *Rheol. Acta*, **13**, 247 (1974).
19. B. Tamamushi, Y. Kodaira, and M. Matsumura, *Colloid Polym. Sci.*, **254**, 571 (1976).
20. T. Yamada and E. Fukada, *Jap. J. Appl. Phys.*, **12**, 68 (1973).
21. E. Kuss, *High Temp.-High Pressures*, **9**, 575 (1977).
22. J. F. Dyre and P. D. Edmonds, *Mol. Cryst. Liq. Cryst.*, **29**, 263 (1975).
23. R. S. Porter, C. Griffin, and J. F. Johnson, *Mol. Cryst. Liq. Cryst.*, **25**, 131 (1974).
24. F. M. Leslie, *Mol. Cryst. Liq. Cryst.*, **7**, 407 (1969).
25. S. Bhattacharga, C. E. Hong, and S. V. Letcher, *Phys. Rev. Lett.*, **41**, 1736 (1978).
26. P. F. Erhardt, J. M. Pochan, and W. C. Richards, *J. Chem. Phys.*, **57**, 3596 (1972).

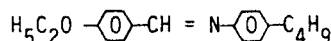
27. J. Pochan, P. Erhardt, and W. C. Richards, *Liq. Cryst. Ordered Fluids*, Vol. 2, eds. J. F. Johnson and R. S. Porter, Plenum Press, New York (1974).
28. I. Janossy, *Ann. Phys.*, (2), 345 (1978).
29. J. L. Ericksen, *Arch. Rat. Mech. Anal.*, 4, 231 (1960).
30. F. M. Leslie, *Quart. J. Mech. Appl. Math.*, 19, 357 (1966).
31. J. Prost, G. Sigand, and B. Regaya, *J. Phys. Lett.*, 37, 341 (1976).
32. F. Jähnig, *Pramana*, 1, 31 (1975).
33. W. H. DeJeu, *Phys. Lett. A*, 69, 122 (1978).
34. A. F. Martins and A. C. Diogo, *Portgal. Phys.*, 9, 129 (1975).
35. P. Martinoty, F. Kiry, S. Nagai, and S. Landau, *J. Phys. (Paris)*, 38, 159 (1977).
36. G. P. MacSithigh and P. K. Currie, *J. Phys. D: Appl. Phys.*, 10, 1471 (1977).
37. H. Imura and K. Okano, *Jap. J. Appl. Phys.*, 11, 1440 (1972).
38. P. E. Cladis and S. Torza, *Phys. Rev. Lett.*, 35, 1283 (1975).
39. Y. R. Lin-Liu, Y. M. Shih, and C.-W. Woo, *Phys. Lett. A*, 57, 43 (1976).
40. Ch., Gahwiller, *Mol. Cryst. Liq. Cryst.*, 20, 301 (1973).
41. A. E. White, P. E. Cladis, and S. Torza, *Mol. Cryst. Liq. Cryst.*, 43, 13 (1977).
42. P. J. Flanders, *Mol. Cryst. Liq. Cryst.*, 29, 19 (1974).
43. C. K. Yun, *Phys. Lett. A*, 369 (1973).
44. S. Meiboom and R. C. Hewitt, *Phys. Rev. Lett.*, 30, 261 (1973).
45. A. Nomura and S. Ogawa, *Jap. J. Appl. Phys.*, 17, 639 (1977).
46. E. Kuss, *Mol. Cryst. Liq. Cryst.*, 47, 71 (1978).
47. P. G. deGennes, *The Physics of Liquid Crystals*, Clarendon Press, Oxford (1974).
48. F. Jähnig and F. Brochard, *J. Physique*, 35, 301 (1974).
49. W. L. McMillan, *Phys. Rev. A*, 9, 1720 (1974).
50. Y. Kawamura and S. Iwayanagi, *Sci. Pap. Inst. Phys. Chem. Res. (Jpn.)*, 70, 38 (1976).
51. Y. Kawamura and S. Iwayanagi, *Mol. Cryst. Liq. Cryst.*, 38, 239 (1977).
52. S. Nagai and K. Iizuka, *Jap. J. Appl. Phys.*, 14, 567 (1975).
53. P. H. Keyes and D. B. Ajgaonkar, *Phys. Lett. A*, 64, 298 (1977).
54. A. F. Martins, A. C. Diogo, and N. PL Vaz, *Ann. Phys.*, (3), 361 (1978).
55. F. Hardouin, M. F. Achard, and G. Sigaud, *J. Phys. Colloq.*, (3), 371 (1979).
56. L. Légere and A. Martinet, *J. Phys., Colloq.*, (3), 89 (1976).

## Appendix

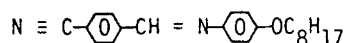
4-methoxybenzylidene-4'-n-butylaniline, MBBA



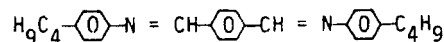
4-ethoxybenzylidene-4'-n-butylaniline, EBBA



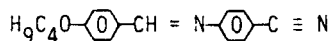
4-cyanobenzylidene-4'-n-octyloxyaniline, CB00A



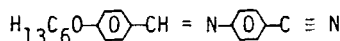
terephthal-bis-butylaniline, TBBA



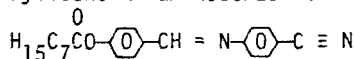
4-n-butoxybenzylidene-4'-aminobenzonitrile



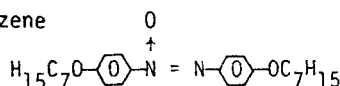
4-n-hexyloxybenzylidene-4'-aminobenzonitrile, HBAB



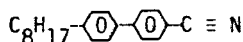
4-n-octanoyloxybenzylidene-4'-aminobenzonitrile



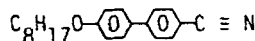
heptyloxyazoxybenzene



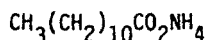
p-n-octyl-p'-cyanobiphenyl



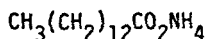
p-n-octyloxy-p'-cyanobiphenyl



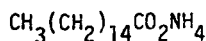
ammonium dodecanoate



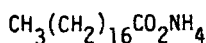
ammonium myristate



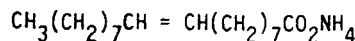
ammonium palmitate



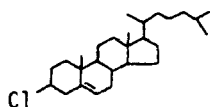
ammonium stearate



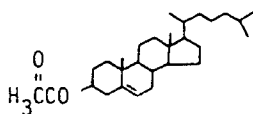
ammonium oleate



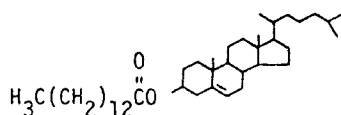
cholesteryl chloride, CCl



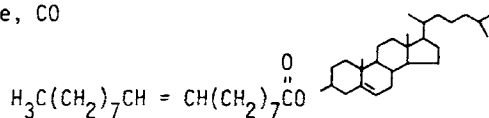
cholesteryl acetate



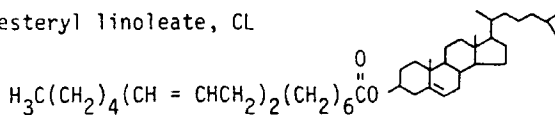
cholesteryl myristate



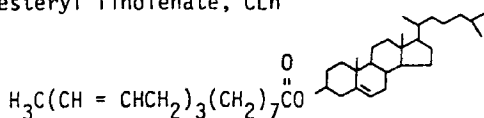
cholesteryl oleate, CO



cholesteryl linoleate, CL



cholesteryl linolenate, CLn



cholesteryl oleyl carbonate, COC

